Silicon resonator sensors: interrogation techniques and characteristics

M.J. Tudor, BSc(Eng)
M.V. Andres, BSc, PhD
K.W.H. Foulds, BSc(Eng), PhD, CEng, FIEE
J.M. Naden, BSc, PhD

Indexing terms: Semiconductor devices and materials, Optical fibres, Optical sensors, Detection, Control equipment and applications

Abstract: Interferometric and noninterferometric optical-fibre sensing systems for resonator vibrations are described. The quality factor variation with pressure, the temperature dependence of resonant frequency and the acceleration sensitivity are given for a double-ended tuning-fork based acceleratometer.

1 Introduction

There is considerable interest, at present, in sensors based on mechanical resonance [1]. The principle of operation is that the resonant frequency is altered by the measurand of interest. The output is a frequency, and thus easily digitised.

One particular class of resonator sensor is made by chemically etching the required geometry in silicon wafers [2]. Many resonators are produced from a single wafer giving low cost and good repeatability. Silicon is a high-strength elastic material which yields by fracturing, rather than plastic deformation, and its single-crystal form implies tolerance of the stress cycling encountered at resonance. Its high purity minimises crack initiation at dislocations and defects, leading to long device lifetimes. The small size of the device, typically 1 cm × 0.5 cm × 0.5 mm, minimises disturbance of the measurand.

Electrical techniques used to sense the vibrations of silicon resonators have used capacitive [3], piezoresistive [4] or magnetic/optical [5] based detection systems. However, for some applications, an optical-fibre based detection system [5] may be desirable. The advantages of optical fibres include intrinsic safety, immunity to electromagnetic interference, corrosion resistance, lightness and the fact that the sensor may easily be remotely operated.

Fibre technology and silicon resonators are compatible in size and can conveniently be combined by using the output of a fibre to sense the vibrations of a resonator. The frequency at which the displacement is largest is the resonant frequency and this is a function of the measurand. This output, being a frequency, is less affected by unintentional light intensity variations which can arise from many sources. Optical-fibre techniques can easily detect the small amplitudes of vibration of silicon resonators which are usually a few micrometres at most.

Additionally, as the resonator's power requirements are low, about 1 mW–1 μW of light guided in the fibre is sufficient to directly excite the vibrations by thermal expansion. One method has used light intensity modulated at the resonant frequency of the sensor [6]. An alternative technique involves self-excitation, and requires only unmodulated light to initiate vibrations which then modulate the light, thus maintaining the vibrations through positive feedback [7]. An important advantage of self-excited sensors is that they yield simple multiplexing schemes because there is no need for an external feedback loop between the sensor and the optical source. An attractive scheme may be based on fibre couplers, using a different frequency band for each sensor and self-excitation of vibrations.

The mechanical performance of a resonator sensor can be described by several key parameters. These include the mode shape, the nonlinearity, the amount of mode coupling, the quality factor Q, the intrinsic sensitivity to temperature and the sensitivity to the measurand. Some of these aspects have already been reported by us. Every frequency-out sensor based on a mechanical resonator exhibits a spectrum of vibrational modes, each mode having its own displacement pattern at resonance. This determines the optimum positions for optical detection and excitation of vibration [6], or alternatively for the location of piezoresistors or capacitative detection. It has also been found that the resonant frequencies can be a function of vibrational amplitude [8]. This nonlinearity has the effect of making a change in the excitation amplitude indistinguishable from a change in the measurand, if only a frequency output is provided. This is clearly undesirable, and so the extent of the nonlinearity must be investigated for each resonator design, to set an upper limit for the amplitude. This upper limit must ensure that any frequency change caused by amplitude changes is small compared with the frequency change caused by the smallest measurand change one wishes to resolve. Another feature that has been observed is possible mode coupling between specific modes in a particular measurand range [9]. Care must be taken in resonator design to ensure that relevant modes do not couple in the measurand range of interest.

This paper deals with, and gives new results for, the other three parameters mentioned earlier, the Q, the

Paper 6178D (C11), received in final form 28th April 1988

M.J. Tudor is with Postal Point 11, Solartron Transducers, Schlumberger Industries, Victoria Road, Farnborough, Hants. GU14 8PW, United Kingdom

M.V. Andres is with the Departmento de Fisica Aplicada, Universitat de Valencia, Burjasot, 46100-Valencia, Spain

K.W.H. Foulds is with the Department of Physics, University of Surrey, Guildford, Surrey GU2 5XF, United Kingdom

J.M. Naden is with STC Technology Ltd., London Road, Harlow, Essex CM17 9NA, United Kingdom

intrinsic temperature sensitivity and the measurand sensitivity. Measurements are made on a specific accelerometer sensor, with its particular geometry, but the results give a good impression of the sensitivity, linearity and dynamic range possible from such devices. First, however, we report on our recent work on optical-fibre interrogation of silicon resonator sensors.

2 Optical fibre detection techniques

Optical-fibre detection techniques may be classified into interferometric techniques, which rely on phase modulation of the optical signal, and noninterferometric techniques, which rely on amplitude modulation. We have previously reported a single-mode fibre based interferometric system [10] and, for convenience, the working principle is described below. We now also report a multimode fibre based interferometric system and an amplitude-modulation based system.

Fig. 1 shows a diagram of the single-mode fibre interferometer developed to sense resonator vibrations. The

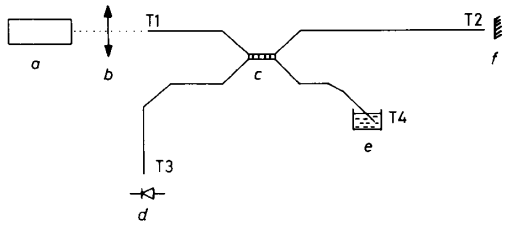

Fig. 1 *Detection system*
(*a*) Source, (*b*) lens, (*c*) coupler, (*d*) detector, (*e*) index matching liquid, (*f*) silicon resonator

heart of the system is a polarisation-independent 3 dB coupler. We assume a signal S incident on T2. At T2, interference occurs between the signal reflected at the end of the fibre rS and the signal cS coupled back into the fibre, from the multireflections taking place in the optical cavity formed by the end of the fibre and the silicon resonator. A complete description must allow for beam divergence within the optical cavity [10]. The resultant reflected signal is given by

$$\Gamma S = rS + cS \tag{1}$$

The power detected at T3 is proportional to $|\Gamma S|^2$, which varies periodically as the distance d from the resonator to T2 is increased, because this changes the phase of c, but tends to $|rS|^2$ for large d because of the beam divergence. There is, therefore, a smooth decrease in the fringe amplitude as d increases. An important criterion for a practical system is that the signal at T3 should be independent of the fibre's optical length, as this can be altered by environmental perturbations. This is achieved because all reflections at T2 follow the same path within the fibre. However, T4 must be index matched to avoid a reflection from this end interfering with the reflections from T2. This would make the interferometer sensitive to differences in the optical length of the arms T2 and T4 and hence changes in the environment, particularly temperature.

Multimode fibre systems still have economic advantages over single-mode systems, particularly with respect to connectors. We have therefore set up the same physical system as that shown in Fig. 1, using multimode fibre and an appropriate coupler, and we shall describe how the operating characteristics differ from those of the single-mode system. Hundreds of modes now travel along the fibre and are incident upon the end of the fibre at T2. For simplicity let us consider just one mode, the mode p, with complex amplitude S_p at T2. This sets up the initial reflected wave $r_p S_p$ at the interface and launches power into the optical cavity creating the multireflected wave. The wave coupled back into the fibre has not only a component in mode p, $c_{pp} S_p$, but also components in other modes, which can now propagate. Thus, the total reflected wave in mode p consists of the initial reflected wave $r_p S_p$ at the interface plus the contributions to mode p from all the other modes, i.e.

$$\Gamma_p S = r_p S_p + c_{pp} S_p + \sum_{q \neq p} c_{pq} S_q \tag{2}$$

For convenience, let us consider just a few modes p, q and r. Over a short enough interval of time, the power flow in mode p is given by

$$W_p = \tfrac{1}{2} | r_p S_p + c_{pp} S_p + c_{pq} S_q + c_{pr} S_r |^2 \tag{3}$$

and the total power received at the detector is the sum of the powers in each of the modes.

The signal coherence plays a vital role in the consequences of eqn. 3. It will be assumed that the coherence length of the source is always appreciably greater than the separation between the end of the fibre at T2 and the silicon resonator. For small separation d, the crosscoupling terms become insignificant and the system produces well defined fringes of interference, even with a large number of modes, because the phase differences between r_p and c_{pp}, r_q and c_{qq} etc. are approximately the same. If the crosscoupling terms are significant and signals S_p, S_q and S_r are coherent, then changing the phase relationships of these signals, by squeezing the fibre, for example, has a critical effect on W_p etc. and is associated with the phenomenon of modal noise [11]. It was found that the effects of the environmental fluctuations modify the fringe amplitude so drastically that the system is useless for reliable measurements, when a high coherence source such as an HeNe laser is used.

If the signals S_p, S_q and S_r are not coherent, and this occurs when the signals have travelled along the fibre a distance greater than $l_c/\Delta n$, l_c being the coherence length of the source and n the difference in the refractive indices of the core and cladding, interference only occurs between the S_p terms in W_p, the S_q terms in W_q etc., the other terms merely contribute to the average intensity. In this case, the fringe amplitude is relatively unaffected by environmental fluctuations or by squeezing the fibre. Fig. 2 shows the variation of the fringe amplitude with d, for a

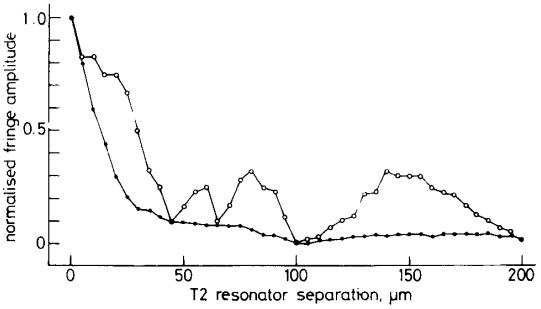

Fig. 2 *Fringe amplitude as a function of fibre resonator separation*
● aligned
○ misaligned

multimode semiconductor laser with a coherence length of about 200 μm normalised to the value at $d = 0$. For the fibre properly aligned perpendicularly to the resonator surface, the fringe amplitude decreases smoothly,

primarily because of the beam-spreading effect, with an indication of periodicity caused by the phase angles of c_{pp}, c_{qq} etc. changing at slightly different rates with d. When the fibre is misaligned, these differences are enhanced and the crosscoupling terms increased, giving rise to a more complicated variation. This also contributes to the reduced fringe amplitude found experimentally, but not revealed in the normalised plot of Fig. 2. Additionally for the multimode system, T4 does not need to be index matched because the phase and amplitude of each mode are different and change with environmental effects compared with the reflections at T2. Hence, the interference between the waves reflected from T2 and T4 averages over the whole fibre to a constant power at the detector. This is a very desirable situation for the multiplex situation mentioned earlier.

Another optical-fibre system that we have also investigated is based on an edge amplitude-modulation technique. The beam is aligned with the edge of the resonator and movement modulates the intensity of light reflected into the fibre. This system is less sensitive to displacement than the interferometric technique. It is desirable to use this system with very low-coherence sources, to avoid the superposition of interferometric fringes on the amplitude modulation. The configuration remains the same as that of Fig. 1 and can be used to detect vibrations parallel or transverse to the fibre axis, with higher sensitivity in the second case.

3 Accelerometer structure and operation

Fig. 3 shows the device geometry of the silicon accelerometer under investigation. The device consists of a surrounding frame from which extend two beams supporting a rectangular slab, which is the inertial mass of the accelerometer. The two supporting beams are about 200 μm thick. Between A and B and in the same plane as the top of the wafer, a resonator is etched. This can be any mechanical element such as a beam or plate, different structures having different properties. In this case, a double-ended tuning fork (DETF) was chosen. A DETF may conveniently be regarded as two tuning forks joined tine to tine, or as two elastically coupled beams. The resonator may vibrate in the Y direction in the XY-plane and in the Z-direction in the XZ-plane. This structure has two major advantages. If large enough displacements are excited, the edge amplitude-modulation optical technique may be used to detect the resonances. If smaller displacements are excited, the interferometric technique may be used to detect the vibrations in the XZ-plane. Hence, the detection technique may be chosen depending on the type and efficiency of the excitation. Secondly, for reasons described later, the structure may exhibit a high Q, in our case a maximum of 7000 in vacuum.

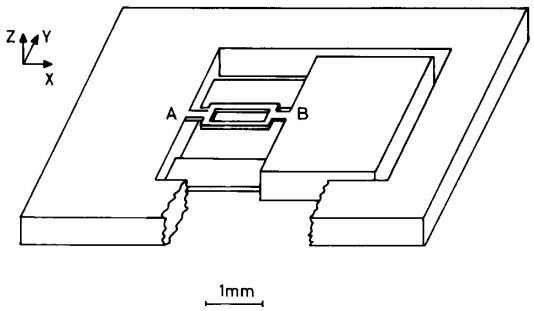

Fig. 3 *Accelerometer geometry*

When the device is subject to an acceleration in the Z-direction, the inertial force on the paddle causes bending of the supports. This bending causes a tensile stress to be applied to the resonator. For a beam, the resonant frequency depends on the applied stress, and, hence, the resonant frequency of the two coupled beams will vary in a similar manner. The DETF can serve as the resonant-stress-sensitive element in any sensor which converts measurand changes to a stress.

For details of resonator manufacturing processes the reader is referred to Reference 2.

4 Quality factor Q

The Q is usually defined as the resonant frequency divided by the bandwidth of the resonance. A high Q is important as it implies better identification of the resonant frequency and, hence, better sensitivity [9]. It also implies low losses from the resonator and, hence, low-power requirements. A resonator acts as a bandpass filter rejecting noise at frequencies outside its bandwidth. A higher Q thus gives better rejection of external noise sources.

The Q is determined by the damping of acoustic waves in the resonator, and several mechanisms of loss have been identified:

(*a*) *Viscous drag and acoustic radiation:* A resonator vibrating in a viscous fluid produces movement of the fluid, with fluid velocity components both parallel and perpendicular to its surface and propagating perpendicular to its surface [12]. Both components give rise to loss, with the production of the perpendicular component, corresponding to acoustic radiation, being efficient and resulting in a low Q when the wavelength of the acoustic waves in the resonator is approximately equal to the acoustic wavelength in the fluid at the frequency of vibration.

(*b*) *Radiation at the supports:* At resonance the vibrations set up a standing-wave pattern within the resonator. However, at the supports or ends of the resonator, some energy is lost outside the resonator decreasing the Q. To avoid this, the motion of the supports should be minimised. For the DETF of Fig. 3, this is achieved in some particular balanced vibrational modes, in which the two beams vibrate in antiphase. The action of one beam at the support is cancelled by the reaction of the other. For the DETF this may occur in either the XZ- or XY-plane. Recent finite-element analyses [13] have provided the optimum DETF geometry to minimise this source of losses.

(*c*) *Internal losses:* These are dependent on the particular material used for the resonator and may be caused by dislocations, scattering from impurities, Akheiser losses and thermoelastic losses. However, silicon normally has a high purity and internal losses are independent of dislocation count below 673°C [14]. Thermoelastic loss is due to irreversible heat conduction, from the regions of compression to the regions of expansion which occur during flexural motion. Akheiser damping occurs because the elastic standing-wave pattern at resonance disturbs the equilibrium distribution of thermally excited elastic waves (phonons).

Removal of the surrounding fluid by vacuum encapsulation eliminates contribution (*a*). Fig. 4 shows the Q-variation as the pressure of the surrounding air is

reduced, and is for a balanced mode of the DETF. Below 40 Pa, Q is constant and is governed by the intrinsic damping of the resonator comprising contributions (*b*)

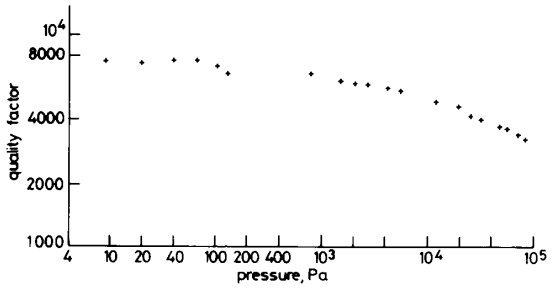

Fig. 4 *Quality factor as a function of the surrounding air pressure*

and (*c*). Newell's model [15] for the viscous drag contribution predicts a faster decrease in the Q than we have measured and also the appearance of a constant Q-region above 400 Pa, governed by the air's viscosity, which we have not observed. Further experiments using specially designed resonators are in progress to study the damping mechanisms.

5 Temperature dependence

The temperature dependence of the resonant frequency of a silicon resonator depends on four major influences:

(i) *Type of vibration:* That is, whether longitudinal, shear, flexural or torsional. This arises as, for each type of vibration, the resonant frequency will depend on different combinations of moduli of elasticity, density, Poisson's ratio and dimensions, each of which will have a different temperature coefficient.

(ii) *Coating on surface of resonator:* Silicon nitride layers may be included on the surface of silicon resonators for passivation [2]. Metallic layers can be deposited to increase the efficiency of optical excitation of vibrations. However, the layer's thermal expansion coefficient will generally differ from that of the silicon resonator, causing either a positive or a negative stress to be generated in the resonator as temperature changes. The sign will depend on the difference in thermal expansion coefficients of the layer and silicon. This stress will modify the temperature dependence and may be used for temperature compensation. It has also been suggested that coating silicon resonators with a material which has a positive temperature coefficient of Young's modulus can also be used to compensate for the temperature dependence of silicon resonators [4].

(iii) *Temperature dependence of mounting:* Unless the resonator is in an all-silicon holder, there will be a differential thermal expansion between the silicon and the mount. The resonator may be subject to a temperature-dependent stress, depending on geometry.

(iv) *Orientation:* It is well known that, in quartz resonators, the temperature dependence is a sensitive function of orientation of the resonator with respect to the crystalline axes. There is a similar effect in silicon, and the temperature-dependence of Young's modulus varies by about 25% along different directions in the (100) plane.

In our experiment the device was mounted so as to eliminate the effect of contribution (iii), and there was no coating so contribution (ii) can be neglected. The resonator length pointed along the crystallographic (110) direction. The mode of vibration was the same as for the Q results of the preceding Section. The vibrations were excited and detected optically. Fig. 5 shows the change in resonant frequency with temperature in the range

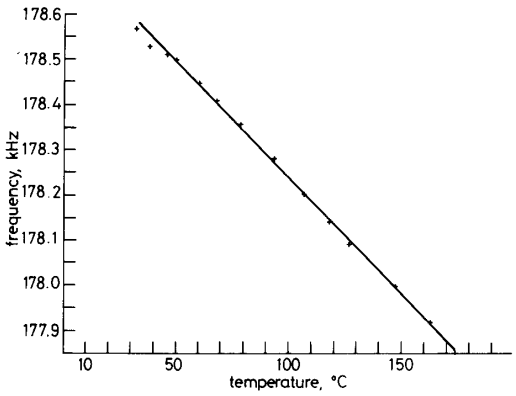

Fig. 5 *Resonant frequency as a function of the device temperature*

30 – 165°C giving an experimental relative change frequency of -29×10^{-6}/°C. To calculate the order of magnitude of the temperature dependence, the vibration of the DETF may be considered as those of two coupled beams, and hence, provided the coupling is temperature-independent, the temperature dependence should be the same as that of a beam in isolation. For a beam in flexural vibration:

$$f_N = C_N \frac{d}{L^2} \sqrt{\frac{E}{\rho}} \tag{4}$$

where f_N is the resonant frequency, C_N is a constant depending on the order of the mode and the end conditions, E is the Young's modulus, ρ is the density, d is the thickness and L is the length.

E, ρ, d and L are temperature-dependent. Differentiating eqn. 4 with respect to temperature and dividing by eqn. 4 gives

$$\frac{1}{f_N}\frac{df_N}{dT} = \frac{1}{2E}\frac{dE}{dT} - \frac{1}{2\rho}\frac{d\rho}{dT} - \alpha \tag{5}$$

where $\alpha = 3 \times 10^{-6}$/°C, the thermal expansion coefficient of silicon and $(1/\rho)(d\rho/dT) = -13 \times 10^{-6}$/°C. $(1/E)(dE/dT)$ is not well established and values between -55×10^{-6}/°C and -113×10^{-6}/°C have been given in earlier publications [16, 17]. This gives an intrinsic temperature dependence in the range -27×10^{-6}/°C to -56×10^{-6}/°C which includes the measured value.

6 Acceleration sensitivity

To measure the acceleration sensitivity, the effect of acceleration has been simulated by suspending weights from the centre of the inertial mass. Fig. 6 shows the effect is linear for small stresses in the range 0–12×10^{-3} kg, and the relative frequency change is 0.483/kg. When the load was increased above 12×10^{-3} kg the DETF broke. This provides a minimum detectable acceleration of 2.5 g, g being 9.8 m/s^2, and a maximum of 1.2×10^3 g. The range is nearly 500 times the minimum detectable acceleration. The sensitivity could be increased by thinning the supports or increasing the inertial mass of the accelerometer, at the expense of a smaller maximum. Dynamically the fundamental resonance of the whole structure is at 3 kHz.

7 Conclusions

It has been demonstrated that a successful interferometric detection system can be constructed using multimode fibre. To minimise the effect of environmental perturbations on the fibre, an optical source with the minimum coherence length to give adequate fringe amplitude should be used.

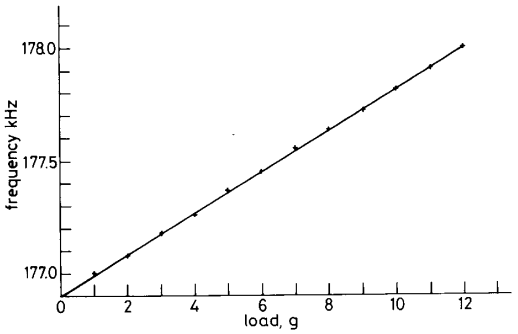

Fig. 6 *Resonant frequency as a function of the applied force*

Among the advantages of the multimode system, we can point out its suitability for coupler-based multiplexing because the reflections from additional resonators and fibre ends will not interfere with each other. However, this could also be accomplished in the single-mode system, by arranging the path difference between successive arms to be greater than the coherence length of the source.

The intrinsic temperature dependence of the sensor is linear over the range room temperature to 160°C, and there is no particular problem optically exciting vibrations at these elevated temperatures. The temperature sensitivity is such that a change of 0.5°C would result in a change in the frequency equal to that caused by the minimum detectable acceleration. Hence, temperature compensation or a parallel temperature measurement is required.

The feasibility of using this device as an accelerometer has been shown, but some extra work on the design has to be carried out in order to modify the operating range and possibly correct the temperature dependence.

8 Acknowledgments

We thank J. Greenwood and P. Hale of STC Technology Ltd., Harlow, for the devices. Acknowledgment is made by Mr. Tudor of an SERC CASE studentship through STC Technology Ltd., Harlow. Dr. Naden is grateful to STC marine systems for permission to publish this paper.

9 References

1 LANGDON, R.M.: 'Resonator sensors — a review', *J. Phys. E*, 1985, **18,** pp. 103–115
2 PETERSON, K.E.: 'Silicon as a mechanical material', *Proc. IEEE*, 1982, **70,** pp. 420–457
3 GREENWOOD, J.C.: 'Etched silicon vibrating sensor', *J. Phys. E*, 1984, **17,** pp. 650–652
4 OTHMAN, M.B., and BRUNNSCHWEILER, A.: 'Electrothermally excited silicon beam mechanical resonators', *Electron. Lett.*, 1987, **23,** (14), pp. 728–730
5 PITT, G.D., EXTANCE, P., NEAT, R.C., BATCHELDER, D.N., JONES, R.E., BARNETT, J.A., and PRATT, R.H.: 'Optical fibre sensors., *IEE Proc. J, Optoelectron.*, 1985, **132,** (4), pp. 214–248
6 ANDRES, M.V., FOULDS, K.W.H., and TUDOR, M.J.: 'Optical activation of a silicon vibrating sensor', *Electron. Lett.*, 1986, **22,** (21), pp. 1097–1099
7 LANGDON, R.M., and DOWE, D.L.: 'Photoacoustic oscillator sensors', *Fibre Optic Sens. 2 Conf.*, The Hague, 30th March–3rd April 1987
8 ANDRES, M.V., FOULDS, K.W.H., and Tudor, M.J.: 'Nonlinear vibrations and hysteresis of micromachined silicon resonators designed as frequency-out sensors', *Electron. Lett.*, 1987, **23,** (18), pp. 952–954
9 ANDRES, M.V., FOULDS, K.W.H., TUDOR, M.J.: 'Sensitivity of a frequency out silicon pressure sensor', *3rd Eurosensors Conf. Sens. & Appl.*, Cavendish Laboratories, Cambridge, 22nd Sept. 1987
10 ANDRES, M.V., TUDOR, M.J., and FOULDS, K.W.H.: 'Analysis of an interferometric optical fibre detection technique applied to silicon vibrating sensors', *Electron. Lett.*, 1987, **23,** (15), pp. 774–775
11 EPWORTH, R.E.: 'The phenomenon of modal noise in fibre systems'. *Fibre Optics Conf.*, Washington, March 1979
12 LANDAU and LIFSHITZ: 'Fluid mechanics' (Pergamon Press, 1959)
13 CLAYTON, L.D., SWANSON, S.R., and EERNISSE, E.P.: 'Modification of the double ended tuning fork geometry for reduced coupling to its surroundings: finite element analysis and experiments', *IEEE Trans.*, 1987, **UFFC-34,** pp. 243–252
14 KLEMENS, P.G.: 'Effect of impurities and phonon processes on the ultrasonic attentuation of germanium, crystal quartz, and silicon', *in* MASON, W.P. (Ed.): 'Physical acoustics—Vol. 3, Pt. B (Academic Press, 1965)
15 NEWELL, W.E.: 'Miniaturisation of tuning forks', *Science*, 1968, **161,** pp. 1320–1326
16 McSKIMIN, H.J.: 'Measurement of the elastic constants at low temperatures by means of ultrasonic waves — data for silicon and germanium single crystals, and for fused silicon', *J. Appl. Phys.*, 1953, **24,** (4), pp. 988–997
17 WEISS, B.L., and SEARS, J.L.: 'Publish and retrieve materials data with EMIS', *IEE Proc. I, Solid-State & Electron. Dev.*, 1981, **128,** (5), pp. 189–191